Space-Range Adaptive Processing for Waveform-Diverse Radar Imaging

Thomas Higgins,[1,2] *Shannon D. Blunt,*[1] *and Aaron K. Shackelford*[2]
[1] EECS Dept. / Radar Systems Lab, University of Kansas, Lawrence, KS
[2] Radar Division, Naval Research Laboratory, Washington, DC

***Abstract*—Waveform-diverse radar arrays have been proposed as a method to facilitate single pulse imaging as well as to potentially enable simultaneous multi-mode operation. Transmitting different waveforms on the elements of a uniform linear array consequently raises the spatial and temporal sidelobes of the receiver matched filter. In this paper a recursive minimum mean square error based receiver design denoted as Space-Range Adaptive Processing is presented. The new method is capable of mitigating space range sidelobes thereby providing enhanced sensitivity for this transmission scheme.**

I. INTRODUCTION

The waveform-diverse array is a conceptual method for spatially distributing energy from a radar antenna array [1-5]. The spatial distribution of energy raises the spatial sidelobes of the matched filter receiver due to the increased energy transmitted in the off-"mainbeam" directions (relative to the standard approach of transmitting an identical waveform on each element). However, the distributed energy allows the radar to simultaneously image/search the illuminated scene as opposed to electronically scanning over the same area. In addition, the added diversity allows the radar to perform different functions in desired directions *e.g.,* emitting communications and electronic attack waveforms while transmitting a sensing waveform in other directions. Recently, a number of approaches have been suggested for waveform diverse array receiver designs within the framework of MIMO radar [6-8].

In this paper a new minimum mean squared error (MMSE) based approach entitled Space-Range Adaptive Processing (SRAP) is applied to the waveform diverse array scenario in an effort to jointly suppress the range and spatial receive sidelobes thus providing enhanced sensitivity for this transmission scheme. SRAP can be viewed as a multi-dimensional extension of Adaptive Pulse Compression (APC) [9] and Re-Iterative Super Resolution (RISR) [10] that addresses the issue of adapting in both the range and spatial dimensions. In addition, multi-dimensional adaptivity facilitates the realization of space-range nulls analogous to space-Doppler nulls demonstrated with Space Time Adaptive Processing (STAP) [11]. Although several similarities can be made to STAP, the SRAP algorithm utilizes a structured covariance matrix to perform scene estimation where as STAP typically relies on a sample covariance matrix formed from measured data to achieve adequate clutter cancellation for moving target indication.

SRAP is an iterative approach that requires an *a priori* estimate of the illuminated scene (*e.g.* via matched filtering). The previous estimate is used to construct a specific filter for each range-angle cell of interest. The set of filters are then applied to yield an improved estimate of the illuminated scene which can subsequently be used to create a new set of filters. The algorithm has been observed to converge after three or four adaptive stages.

II. SPACE-RANGE ADAPTIVE PROCESSING

A. Signal model

The waveforms transmitted from an M element uniform linear array can be represented as the $N \times M$ matrix $\mathbf{S}$ of which the m^{th} column contains the length-N discretized waveform transmitted from the m^{th} element of the array. Note that for traditional beamforming the columns of $\mathbf{S}$ would be identical aside from the elemental phase shift used for transmit beam-steering.

The discretized model for the received signal from the ℓ^{th} range cell on the M elements of a waveform-diverse uniform linear array can be denoted as the $1 \times M$ vector

$$\mathbf{y}(\ell) = \left[\sum_{\theta} \mathbf{x}^T(\ell,\theta) \mathbf{S} \mathbf{v}_\theta \mathbf{v}_\theta^T \right] + \mathbf{z}(\ell), \qquad (1)$$

in which $(\bullet)^T$ is the transpose operation, $\mathbf{x}(\ell,\theta) = \left[x(\ell,\theta) \;\; x(\ell-1,\theta) \;\; \cdots \;\; x(\ell-N+1,\theta) \right]^T$ is a collection of the complex scattering coefficients associated with the scatterers in the range profile corresponding to angle θ with which the M waveforms convolve at delay ℓ, $\mathbf{v}_\theta = \left[1 \;\; e^{j\pi\sin\theta} \;\; e^{j2\pi\sin\theta} \;\; \cdots \;\; e^{j(M-1)\pi\sin\theta} \right]^T$ is the steering vector associated with spatial angle θ under the assumption

This work was sponsored by the Office of Naval Research base program, the Radar Division of the Naval Research Laboratory, and the Air Force Office of Scientific Research.

Report Documentation Page

Form Approved
OMB No. 0704-0188

1. REPORT DATE	2. REPORT TYPE	3. DATES COVERED
MAY 2010		**00-00-2010 to 00-00-2010**

4. TITLE AND SUBTITLE	5a. CONTRACT NUMBER
Space-Range Adaptive Processing for Waveform-Diverse Radar Imaging	5b. GRANT NUMBER
	5c. PROGRAM ELEMENT NUMBER
6. AUTHOR(S)	5d. PROJECT NUMBER
	5e. TASK NUMBER
	5f. WORK UNIT NUMBER
7. PERFORMING ORGANIZATION NAME(S) AND ADDRESS(ES) **Naval Research Laboratory,Radar Division,Washington,DC,20375**	8. PERFORMING ORGANIZATION REPORT NUMBER
9. SPONSORING/MONITORING AGENCY NAME(S) AND ADDRESS(ES)	10. SPONSOR/MONITOR'S ACRONYM(S)
	11. SPONSOR/MONITOR'S REPORT NUMBER(S)

12. DISTRIBUTION/AVAILABILITY STATEMENT
Approved for public release; distribution unlimited

13. SUPPLEMENTARY NOTES
See also ADM002322. Presented at the 2010 IEEE International Radar Conference (9th) Held in Arlington, Virginia on 10-14 May 2010. Sponsored in part by the Navy.

14. ABSTRACT
Waveform-diverse radar arrays have been proposed as a method to facilitate single pulse imaging as well as to potentially enable simultaneous multi-mode operation. Transmitting different waveforms on the elements of a uniform linear array consequently raises the spatial and temporal sidelobes of the receiver matched filter. In this paper a recursive minimum mean square error based receiver design denoted as Space-Range Adaptive Processing is presented. The new method is capable of mitigating space range sidelobes thereby providing enhanced sensitivity for this transmission scheme.

15. SUBJECT TERMS

16. SECURITY CLASSIFICATION OF:			17. LIMITATION OF ABSTRACT	18. NUMBER OF PAGES	19a. NAME OF RESPONSIBLE PERSON
a. REPORT	b. ABSTRACT	c. THIS PAGE			
unclassified	**unclassified**	**unclassified**	**Same as Report (SAR)**	**6**	

of $\lambda/2$ element spacing, and $\mathbf{z}(\ell)$ is a $1\times M$ vector of additive noise samples.

The collection of N temporal snapshots of (1) can be expressed as

$$\mathbf{Y}(\ell)=\left[\sum_{\theta}\mathbf{X}(\ell,\theta)\mathbf{S}\mathbf{v}_{\theta}\mathbf{v}_{\theta}^{T}\right]+\mathbf{Z}(\ell), \qquad (2)$$

where

$$\mathbf{X}(\ell,\theta)=\begin{bmatrix} x(\ell,\theta) & x(\ell-1,\theta) & \cdots & x(\ell-N+1,\theta) \\ x(\ell+1,\theta) & x(\ell,\theta) & \cdots & x(\ell-N+2,\theta) \\ \vdots & \vdots & \ddots & \vdots \\ x(\ell+N-1,\theta) & x(\ell+N-2,\theta) & \cdots & x(\ell,\theta) \end{bmatrix} \qquad (3)$$

contains the complex amplitudes of scatterers within $2N-1$ range cells of $x(\ell,\theta)$. The final space-range signal model is a reorganized version of (2) and is expressed as the $NM\times 1$ vector

$$\tilde{\mathbf{y}}(\ell)=\left[\sum_{\theta}\mathbf{X}(\ell,\theta)\mathbf{S}\mathbf{v}_{\theta}\otimes\mathbf{v}_{\theta}\right]+\tilde{\mathbf{z}}(\ell), \qquad (4)$$

where $\otimes$ denotes the Kronecker product and $\tilde{\mathbf{z}}(\ell)=\mathrm{vec}\left(\mathbf{Z}^{T}(\ell)\right)$. Using the formulation in (4), the application of a space-range matched filter takes the form

$$\hat{x}_{\mathrm{MF}}(\ell,\theta)=\left(\mathbf{S}\mathbf{v}_{\theta}\otimes\mathbf{v}_{\theta}\right)^{H}\tilde{\mathbf{y}}(\ell), \qquad (5)$$

in which $(\bullet)^{H}$ denotes the complex-conjugate transpose (or Hermitian) operation. Likewise, the SRAP estimate can be obtained by applying the adaptive filter $\mathbf{w}(\ell,\theta)$ as

$$\hat{x}_{\mathrm{SRAP}}(\ell,\theta)=\mathbf{w}(\ell,\theta)^{H}\tilde{\mathbf{y}}(\ell), \qquad (6)$$

which is derived in the following section.

B. Space-Range Adaptive Processing

The MMSE cost function for the complex amplitude in the range-angle cell corresponding to delay ℓ and spatial angle θ is given as

$$J(\ell,\theta)=E\left[\left|x(\ell,\theta)-\mathbf{w}^{H}(\ell,\theta)\tilde{\mathbf{y}}(\ell)\right|^{2}\right], \qquad (7)$$

where $E[\bullet]$ is the expectation operator and $\mathbf{w}(\ell,\theta)$ is the adaptive filter for the (ℓ,θ) range-angle cell. Minimization of (7) with respect to $\mathbf{w}^{*}(\ell,\theta)$ yields

$$\mathbf{w}(\ell,\theta)=\left(E\left[\tilde{\mathbf{y}}(\ell)\tilde{\mathbf{y}}^{H}(\ell)\right]\right)^{-1}E\left[x^{*}(\ell,\theta)\tilde{\mathbf{y}}(\ell)\right], \qquad (8)$$

in which $(\bullet)^{*}$ denotes complex conjugation.

Assuming the range-angle cells are uncorrelated with each other and with the noise, the filter in (8) can be expressed as

$$\mathbf{w}(\ell,\theta)=\rho(\ell,\theta)\left(\sum_{\phi}\left(\mathbf{R}(\ell,\phi)\otimes\mathbf{v}_{\phi}\mathbf{v}_{\phi}^{H}\right)+\mathbf{R}_{\mathrm{Z}}(\ell)\right)^{-1}\mathbf{S}\mathbf{v}_{\theta}\otimes\mathbf{v}_{\theta}, \qquad (9)$$

where $\rho(\ell,\theta)=E\left[\left|x(\ell,\theta)\right|^{2}\right]$ is the power in the range-angle cell corresponding to delay ℓ and spatial angle θ, $\mathbf{R}_{\mathrm{Z}}(\ell)=\sigma_{\mathrm{Z}}^{2}\mathbf{I}_{NM\times NM}$ is the noise covariance matrix under the assumption of white noise (where σ_{Z}^{2} is the noise power), and

$$\mathbf{R}(\ell,\phi)=\sum_{n=-N+1}^{N-1}\rho(\ell+n,\phi)\mathbf{t}_{\phi,n}\mathbf{t}_{\phi,n}^{H}, \qquad (10)$$

where

$$\mathbf{t}_{\phi,n}=\begin{cases}\left[t_{\phi}(|n|)\ \cdots\ t_{\phi}(N-1)\ \mathbf{0}_{1\times|n|}\right]^{T} & \text{for}\quad n\le 0\\ \left[\mathbf{0}_{1\times n}\ t_{\phi}(0)\ \cdots\ t_{\phi}(N-1-n)\right]^{T} & \text{for}\quad n>0\end{cases} \qquad (11)$$

consists of shifted versions of the composite waveform transmitted in the ϕ direction according to $\mathbf{S}\mathbf{v}_{\phi}$. Note that due to the inherent transmit coupling of space and range, the composite waveform is different for different spatial transmit directions. Additionally a normalization procedure, similar to that used in [12], is applied to the filter in (9) yielding

$$\tilde{\mathbf{w}}(\ell,\theta)=\frac{\mathbf{w}(\ell,\theta)}{\mathbf{w}^{H}(\ell,\theta)\left(\mathbf{S}\mathbf{v}_{\theta}\otimes\mathbf{v}_{\theta}\right)}\sqrt{\frac{G}{\left(\mathbf{S}\mathbf{v}_{\theta}\otimes\mathbf{v}_{\theta}\right)^{H}\left(\mathbf{S}\mathbf{v}_{\theta}\otimes\mathbf{v}_{\theta}\right)}}, \qquad (12)$$

in which $G=\max_{\theta}\left[\left(\mathbf{S}\mathbf{v}_{\theta}\otimes\mathbf{v}_{\theta}\right)^{H}\left(\mathbf{S}\mathbf{v}_{\theta}\otimes\mathbf{v}_{\theta}\right)\right]$. This normalization alleviates gain variations among the set of range-angle filters thus resulting in improved performance and robustness to high dynamic range scenarios.

III. IMPLEMENTATION

SRAP utilizes a recursive MMSE structure to alternate between estimating range-angle specific filters and the range-angle scattering coefficients of the illuminated area. A block diagram depicting the implementation of the SRAP algorithm is shown in Fig. 1. The matched filter from (5) can be used to obtain an initial estimate of the scattering coefficients which are then used to construct the covariance matrix in (10) for each cell needed to form the corresponding adaptive filter. The new estimates obtained by applying these unique range-angle filters can be utilized to update the signal covariance matrix after which a new set of filters can be computed and applied. The algorithm generally converges after three or four adaptive stages.

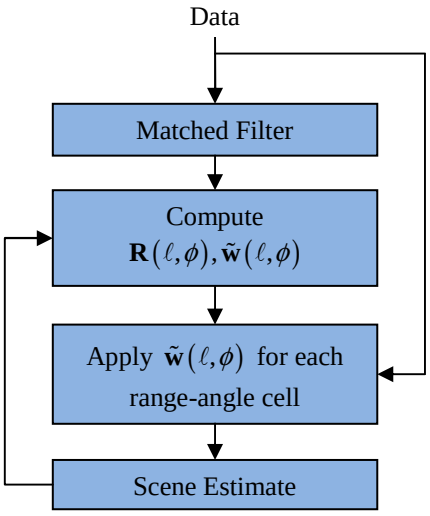

Figure 1. Block diagram of SRAP implementation

IV. TRANSMISSION SCHEME

Several approaches have been examined to optimally achieve a desired transmit beampattern via waveform diversity [13-15]. In this paper we employ a simple yet effective beam spoiling technique. However it should be noted that improvements in the characteristics of the transmitted waveforms, *i.e.*, low range/spatial sidelobes, will yield enhanced sensitivity in the receiver output for both the matched filter and SRAP. Here, waveform multiplexing and an intra-pulse steering will be utilized to create a spoiled transmit beampattern. This technique allows the user to define a set of K angle-specific waveforms where the k^{th} length-N/K waveform is denoted $\tilde{\mathbf{s}}_k$ and θ_k is the associated angle. The initial step in this particular scheme is to interleave the desired waveform set in a time-division multiple-access (TDMA) format [16] and repeat the sequence to form a matrix in which each column is associated with the transmitted waveform on the corresponding antenna element denoted as

$$\tilde{\mathbf{S}} = \text{vec}\left(\begin{bmatrix} \tilde{\mathbf{s}}_0^T \\ \tilde{\mathbf{s}}_1^T \\ \vdots \\ \tilde{\mathbf{s}}_{K-1}^T \end{bmatrix}_{K\times\frac{N}{K}}\right)\begin{bmatrix}1 & 1 & \cdots & 1\end{bmatrix}_{1\times M}. \qquad (13)$$

Next, intra-pulse steering is applied to $\tilde{\mathbf{S}}_{N\times M}$ which imposes the corresponding elemental phase-shift associated with each of the multiplexed waveforms denoted as

$$\mathbf{S} = \tilde{\mathbf{S}}_{N\times M} \odot \exp\left(j\left(\begin{bmatrix} \mathbf{I}_{K\times K} \\ \mathbf{I}_{K\times K} \\ \vdots \\ \mathbf{I}_{K\times K} \end{bmatrix}_{N\times K}\begin{bmatrix} \pi\sin\theta_0 \\ \pi\sin\theta_1 \\ \vdots \\ \pi\sin\theta_{K-1} \end{bmatrix}\begin{bmatrix}0 & 1 & \cdots & M-1\end{bmatrix}\right)\right). \qquad (14)$$

Traditionally a linear phase shift is induced between array elements over an entire pulse to transmit energy in a single direction whereas in (14) the elemental phase shift is altered multiple times during the pulse to steer different portion of the temporal waveform in different spatial directions. Note that each discrete sample of an underlying waveform $\tilde{\mathbf{s}}_k$ is transmitted in the same direction. The spatio-temporal structure of the transmitted signals may potentially enhance cooperative passive bistatic radar while complicating passive exploitation.

The transmit strategy can be characterized in terms of an aggregate beampattern [13] denoted as

$$B(\theta) = \mathbf{v}_\theta^H \mathbf{S}^H \mathbf{S}\mathbf{v}_\theta, \qquad (15)$$

which can be decomposed into the contributions from each temporal sample of $\mathbf{S}$ resulting in the instantaneous time-varying beampattern

$$B_{TV}(n,\theta) = \mathbf{v}_\theta^H \bar{\mathbf{s}}_n \bar{\mathbf{s}}_n^H \mathbf{v}_\theta, \qquad (16)$$

where $\bar{\mathbf{s}}_n$ is the n^{th} column of $\mathbf{S}^T$. Note that the structure employed in (13) and (14) can be augmented to create several different beampatterns.

As an example, consider a $M = 20$ element uniform linear array with $K = 10$ waveforms of length-$N/K = 20$ (thus 10 different spatial beams will be formed during the pulse interval). In this example the waveforms $\tilde{\mathbf{s}}_k$ are unique random polyphase codes and $\theta_k = -30^\circ + \left(60^\circ/9\right)k$ for $k = 0,\cdots,K-1$. The resulting aggregate and time-varying beampatterns are shown in Figs. 2 and 3, respectively. Both beampatterns are peak-normalized to unity.

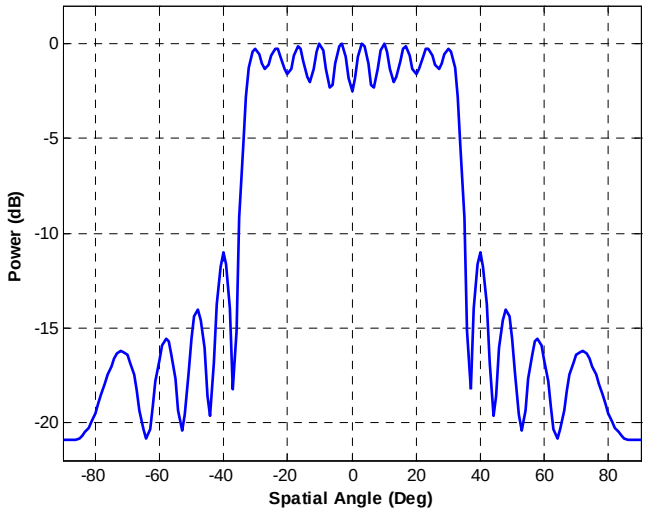

Figure 2. Aggregate beampattern for waveform diverse array example

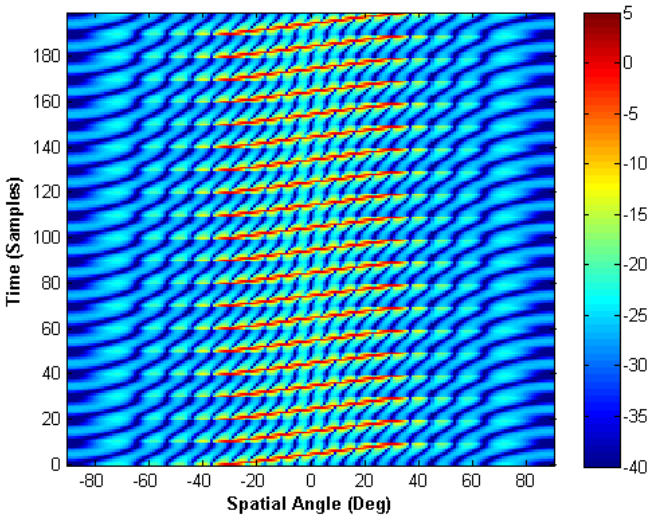

Figure 3. Time-varying transmit beampattern in dB for waveform diverse array example

V. Simulation Results

Again consider an $M = 20$ element uniform linear array with half-wavelength spacing. For this case the transmitted waveforms are those described in the previous section. First an imaging scenario will be inspected and then a surveillance setting containing multiple targets distributed in range and angle will be examined. In all cases the scatterers are modeled as point targets with random phase and amplitude in additive white Gaussian noise. The scenes are constructed using 181 spatial bins distributed evenly between $\pm 90^{o}$ relative to boresight. The matched filter and SRAP will utilize 91 spatial bins evenly distributed between $\pm 90^{o}$ relative to boresight for processing. Note that the illuminated scenes will contain targets that lie between the spatial directions considered for processing resulting in spatial steering vector mismatch. A post-processing equalization is applied to both the matched filter and SRAP estimates to remove the weighting imposed by the transmit beampattern. Note that all images are normalized by the processing gain and presented in dB.

Figure 4 displays the ground truth for the imaging case which consists of several closely spaced shapes. Before processing the SNR of the shapes range from -12 dB to 0 dB (the total processing gain is 26 dB). The matched filter output in Fig. 5 is plagued with space-range sidelobes thereby resulting in a very poor image. In contrast, Fig. 6 displays the SRAP output which has suppressed nearly all of the space-range sidelobes to the level of the noise. A total of four adaptive stages were utilized to produce the image in Fig. 6.

The "one size fits all" approach of deterministic filtering attempts to construct a filter that is appropriate for all scenarios, typically by minimizing the peak or average sidelobe level. In contrast, the adaptive filter structure allows a unique filter to be designed for each range-angle cell based on an estimate of the surrounding scatterers. This approach alleviates the constraints on the filter by requiring only enhanced performance for the particular scenario corresponding to each filter's location. For example, Fig. 7 displays the peak-normalized range-angle response for the SRAP filter from range cell 215 and angle 0^{o} after the final stage. The filter response indicates the output of a specific filter when multiplied by delayed versions of the spatial steering vectors. Notice the space-range nulls at the range and angle offsets corresponding to the surrounding scatterers thus demonstrating the ability of SRAP to manipulate the available degrees of freedom to reduce contributions from range/spatial sidelobes where appropriate. Note that the filter response still contains sidelobe levels near that of the matched filter response. However, the SRAP filter's sidelobes reside in locations that correspond to regions of the scene that do not contain any large scatterers and thus do not impact performance.

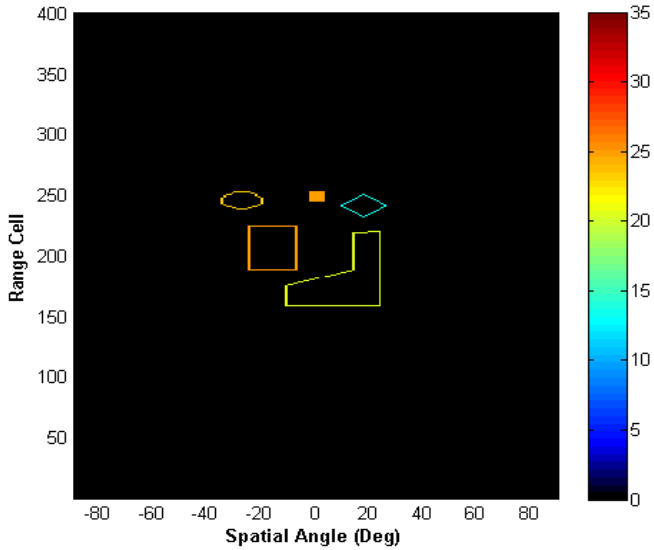

Figure 4. Ground truth for imaging scenario

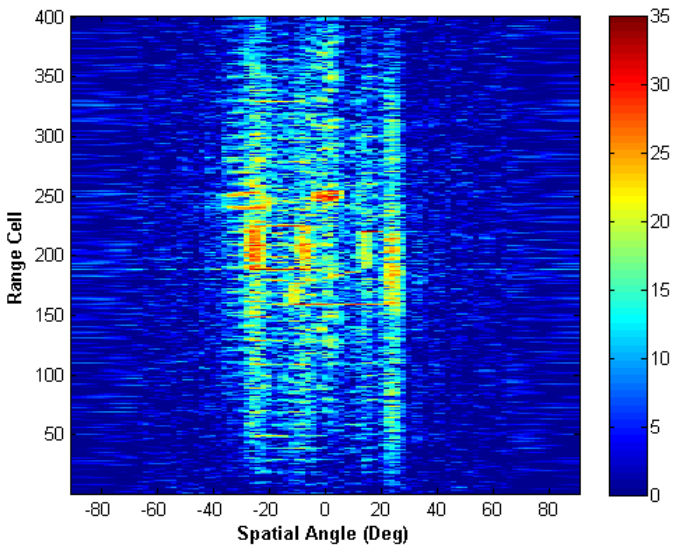

Figure 5. Matched filter estimate for imaging scenario

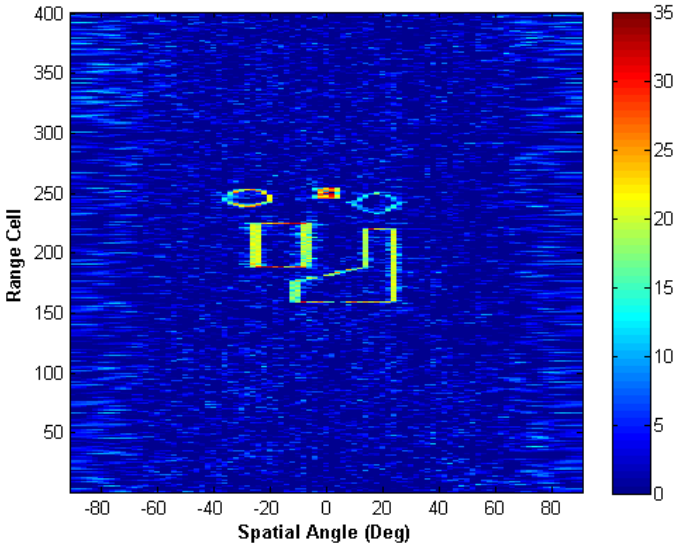

Figure 6. SRAP estimate for imaging scenario

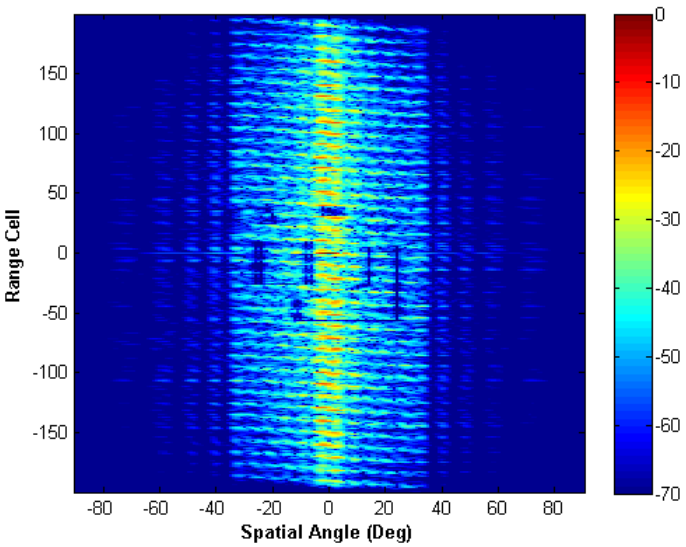

Figure 7. SRAP filter response for imaging scenario (constructed with the adaptive filter from $\ell = 215$, $\theta = 0^{o}$)

The radar parameters for the second scenario are the same as before but the illuminated scene now contains 9 distributed targets between range cells 125 and 175 and angles -30^{o} and $+30^{o}$ as described in Table 1 (stated SNR values are before processing). After processing the SNR of the largest target is 35 dB. Similar to the previous case the matched filter results in limited sensitivity as illustrated in Fig. 8, in which it is difficult to separate the targets, whose locations are denoted by the white circles, from the sidelobes. Figure 9 displays the result after three adaptive stages of SRAP resulting in complete sidelobe mitigation thus revealing all 9 targets. The output power levels in Figs. 8 and 9 are normalized by the processing gain such that the output noise power is approximately 0 dB. This particular mode enables wide area coverage for a sustained period of time thus allowing for inverse synthetic aperture imaging to be accomplished at the same time as detection and tracking operations. It should be noted that different types of waveforms (*e.g.* track, search, imaging) can be transmitted simultaneously using the transmission scheme presented here.

TABLE 1. TARGET DESCRIPTION FOR SURVEILLANCE SCENARIO

Range Cell	Angle (Deg)	SNR (dB)
126	–21	-10
129	0	9
137	–26	–9
141	–3	–11
144	20	7
146	26	–11
148	13	–8
157	–10	–10
161	–20	4

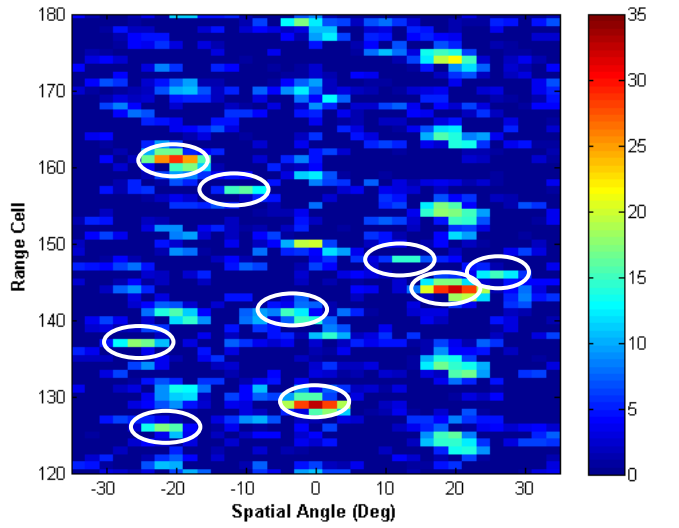

Figure 8. Matched filter estimate for surveillance scenario

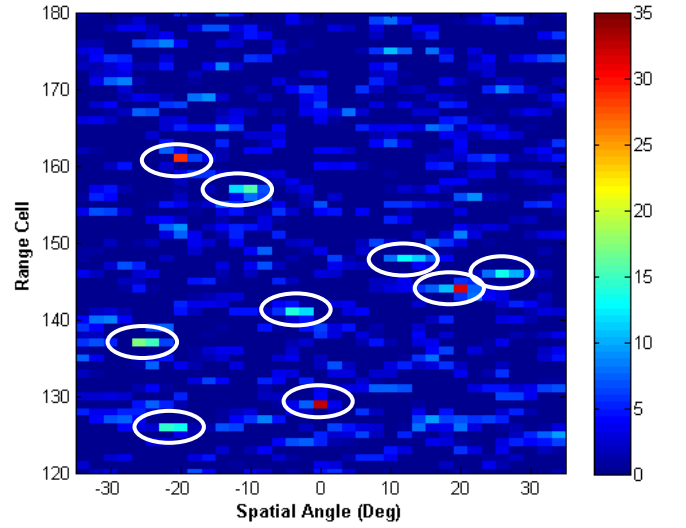

Figure 9. SRAP estimate for surveillance scenario

The closely related one-dimensional MMSE spatial estimation technique RISR is capable of achieving finer resolution than the matched filter, thus we expect to see similar performance from the coupled domain processor SRAP. After examining the spatial extent of the targets in Figs. 7 and 8 it appears that SRAP achieves a finer angular resolution than the matched filter, however full evaluation on the super-resolution capabilities of the algorithm is left as future work. Additionally, in Fig. 7 some of the targets do not fall on the spatial sampling grid used for processing (targets with odd angle values in Table 1) resulting in spatial steering vector mismatch. However, the SRAP algorithm is still effective at suppressing the sidelobes of these targets.

VI. CONCLUSIONS

A new minimum mean squared error (MMSE) based technique denoted as Space-Range Adaptive Processing (SRAP) has been proposed that is capable of mitigating the joint space-range sidelobes inherent to waveform-diverse arrays. In the spirit of the well known STAP formulation, SRAP utilizes a range-angle coupled signal model allowing for simultaneous adaptation in the spatial and range dimensions. SRAP has been shown to exhibit enhanced sensitivity when compared to the matched filter. In combination with the transmission scheme presented here, SRAP facilitates the potential realization of some forms of simultaneous multi-mode operation.

REFERENCES

[1] P.Antonik, M.C. Wicks, H.D. Griffiths, C.J. Baker, "Range-dependent beamforming using element level waveform diversity", *2nd International Waveform Diversity and Design Conference*, Lihue, HI, Jan. 22-27, 2006.

[2] P.Antonik, M.C. Wicks, H.D. Griffiths, C.J. Baker, "Multi-mission multi-mode waveform diversity", *IEEE Radar Conference*, pp. 580-582, Verona, NY, Apr 24-27, 2006.

[3] M. Secmen, S. Demir, A. Hizal, T. Eker, "Frequency diverse array antenna with periodic time modulated pattern in range and angle", *IEEE Radar Conference*, pp. 427 – 430, Waltham, MA, Apr. 17-20, 2006.

[4] Baizert P., Hale T.B., Temple M.A., Wicks, M.C., "Forward-looking radar GMTI benefits using a linear frequency diverse array", *IEE Electronics Letters*, vol. 42, no. 22, pp. 1311 – 1312, Oct 2006.

[5] T. Higgins and S.D. Blunt, "Analysis of range-angle coupled beamforming with frequency-diverse chirps", *4th International Waveform Diversity and Design Conference*, pp. 140 – 144, Orlando, FL, Feb 9-13, 2009.

[6] W. Roberts, J. Li, P. Stoica, and X. Zhu, "MIMO radar reciever design", *4th International Waveform Diversity and Design Conference*, Orlando, FL, Feb 9-13, 2009.

[7] W. Roberts, T. Yardibi, J. Li, X. Tan, and P. Stoica, "Sparse signal representation for MIMO radar imaging," *42nd Asilomar Conference on Signals, Systems and Computers*, pp. 609 – 613, Pacific Grove, CA, October 2008.

[8] W. Roberts, J. Li, P. Stoica, T. Yardibi, and F.A. Sadjadi, "MIMO radar angle-range-Doppler imaging," *IEEE Radar Conference*, Pasadena, CA, May 4-8 2009.

[9] S.D. Blunt and K. Gerlach, "Adaptive pulse compression via MMSE estimation," *IEEE Trans. Aerospace and Electronic Systems*, vol 42, no. 3, pp. 1043-1057, Jan. 2006.

[10] S.D. Blunt, T. Chan, and K. Gerlach, "A new framework for direction-of-arrival estimation," *IEEE Sensor Array and Multichannel Signal Processing Workshop*, pp. 81-85, Darmstadt, Germany, July 21-23, 2008.

[11] J. Ward, "Space-time adaptive processing for airborne radar systems," Lincoln Lab Tech Report 1015, Dec. 13, 1994

[12] T. Higgins, S.D. Blunt, and K. Gerlach, "Gain-constrained adaptive pulse compression via an MVDR framework," *IEEE Radar Conference*, Pasadena, CA, May 4-8 2009.

[13] P. Stoica, J. Li, and Y. Xie, "On probing signal design for MIMO radar," *IEEE Trans. Signal Processing*, vol 55, no. 8, pp. 4151-4161, Jan. 2008.

[14] D. Fuhrmann, J.P. Browning, and M. Rangaswamy, "Constant-modulus partially correlated signal design for uniform linear and rectangular MIMO radar arrays", *4th International Waveform Diversity and Design Conference*, pp. 197 – 201, Orlando, FL, Feb 9-13, 2009.

[15] D. Fuhrmann, and G. San Antonio, "Transmit beamforming for MIMO radar systems using signal cross correlation," *IEEE Trans. Aerospace and Electronic Systems*, vol 44, no. 1, pp. 171-186, Jan. 2008.

[16] T.S. Rappaport, *Wireless Communications Principles and Practice*, Prentice Hall, 1996, pp. 400-404